Dynamics of Continuous, Discrete and Impulsive Systems
Series **A:** *Mathematical Analysis* **16 (2009)** 863-890
 http://www.watam.org

A NEW APPROACH TO CHAOS

Ray Brown[1] and Vivek Jain.[2]

[1]The EASI Academy
Falls Church, Virginia, USA

[2]George Washington University Medical School
The George Washington University, Washington D. C., USA

Abstract. It is well known that chaotic systems have unpredictable time series, exponentially sensitive dependence on initial conditions, a noisy spectrum, and various other properties of pseudo-random processes. These properties have made it difficult to analyze and understand chaotic systems using traditional approaches to the study of differential equations. In this paper we present a new approach to chaos. This approach is suggested by the most complex chaotic system known, the human EEG. We argue that chaotic systems, and complex systems generally, may be better approached by understanding their morphology as is done by physicians when inspecting the human EEG. From a morphological point-of-view, the complex, pseudo-random properties of chaotic time series are not an obstacle to understanding chaos or formulating applications of chaos. But to be mathematically and scientifically rigorous, this view requires that we formalize the concept of morphology and understand the source(s) of the morphology of chaotic systems. In this paper, we offer a formal definition of morphology and examine the sources of morphology for a class of ODE's with chaotic solutions. To support the development of a morphological approach, we turn to the concept of *Dynamical Synthesis* [6]. This is an approach that requires us to reverse engineer complex dynamics as opposed to deriving equations from the laws of science. Specifically, to achieve dynamical synthesis we must learn what are the building blocks of complex systems by first examining and dissecting many mathematical system that exhibit complex properties, and then derive the fundamental theorems that guide the use of the building blocks to construct models and carry out predictions. To initiate this program we first examine the source of complexity in chaotic systems and then derive three methods to generate this complexity; the third method derives almost periodic functions that have the properties of unstable manifolds.

Keywords. Chaos, EEG, EKG, morphology, complexity, dynamical synthesis.

AMS (MOS) subject classification: 37D45.

1 Introduction

The phenomena of chaos has been known since the work of Poincaré[13]. Without the aid of modern computers, Poincaré correctly analyzed the source of this complexity, illustrated with time-one maps in Fig.1, see [12] for details of how figures of unstable manifolds are derived.

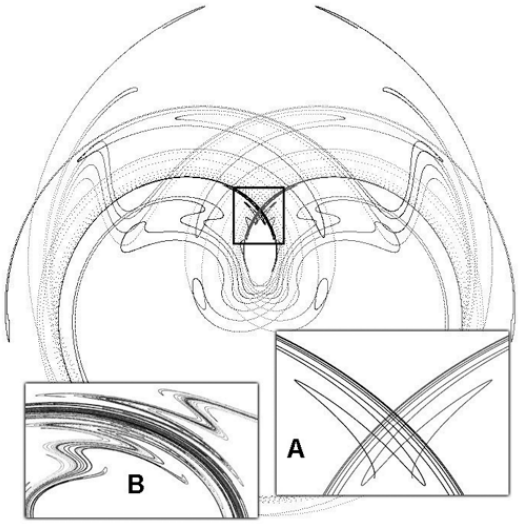

Figure 1: In this figure we see both stable and unstable manifolds, which are symmetric for the twist-and-flip map. The trellis referred to by Poincaré [13] is further designated by the white box and is enlarged in A. In B, the unstable manifold in the vicinity of the fixed point is shown in more detail.

Its complexity, while clearly understood by Poincaré, was formally characterized by Smale [14] in the Smale-Birkhoff theorem. What was revealed by the Smale-Birkhoff theorem was that chaotic systems can behave like random phenomena even though their time series arises from the solution of a deterministic ODE. Since the early 80's, it has been the topic of thousands of articles and research projects, yet, wide-spread use of chaos in industry is limited and somewhat focused on controlling chaos. Most applications center on using some form of fractional dimension or correlation coefficient to measure the extent of the complexity of a given chaotic system. The reason for the limited progress in applying chaos is characterized by the following question: "How do we construct useful applications of a class of systems which are inherently unpredictable"? In this paper we present a new way to understand and approach chaos that may lead to the possibility for significant applications. To have a guide to follow in this discussion of chaos, we turn to the most complex chaotic system we know: the human brain. Within the dynamics of the human brain we turn to the human EEG.

Following the model of how physicians use the EEG to identify neurological abnormalities, we suggest that it is possible that chaos can be understood morphologically. This approach is forced on the physician due to the difficulty of understanding the EEG mathematically. In order to see how to approach chaotic time series morphologically, we turn to chaotic systems

with discrete forcing functions or transition functions (defined below) to provide a clue to the source of the morphology of chaotic systems. The simplest starting point is nonlinear ODE's with discrete forcing. From a morphological point-of-view, it is unimportant that the future of a chaotic time series is uncorrelated to its past, or that two time series from very close initial conditions become uncorrelated. It is only important to know 'approximately' what family of curves the chaotic system uses to produce the morphology of the time series and to understand the conditions under which it moves through this family of curves.

2 The EEG Model of Chaos

As noted in the introduction, what has led to our focus on morphology is an examination of the human EEG. A single observation about the human sleep EEG provides the clue we are seeking: While every human brain is different and the 'mesoscopic' mechanisms that produce electrical activity in the brain may vary to some degree as well (since the each human brain is not a cookie cutter copy of some reference brain) the morphological presentation of normal brain EEG's is still very similar in the eyes of neurologists. Thus, the chaotic mechanisms in all normal human brains must be similar to one another but need not, and cannot, be exactly the same as would be the case if brains were made from a reference, or standard, brain.

How this can happen is illustrated by the Chua circuit analysis found in [1]. As shown there, and in Figure 2, one can mathematically construct an infinity of double scrolls without reference to the Chua circuit. They will all be different from the Chua double scroll but similar enough to produce similar morphologies and 'statistically' similar dynamics. In the same paper we show how to construct Lorenz analogs and Rössler analogs in abundance, all being statistically and morphologically similar to the Lorenz and Rössler systems, but not exact replications. Further, if we look at the time series for the Chua, Lorenz or Rössler equations, and compare them to mathematically constructed analogs following the methods in [1] they will all have different time series from their more famous progeny, but the morphological characteristics will be the very similar, just as we see in the human EEG. Thus, it is the morphology of the time series that is the relevant invariant rather than its specific time series values. For every initial condition, the morphology of the Chua circuit is 'nearly' the same, as is true of Lorenz and Rössler. Likewise, if we follow the construction found in Brown [1] the morphology of a mathematically constructed, rather than a derived, equation, whether it be of the Chua type, Lorenz type, or the Rössler type, the morphology will follow that of the Chua, Lorenz, and Rössler respectively. By delay plots and other devices, it is possible to identify these systems from samples of their time series, just as physicians do with the human EEG, and then reverse engineer the system from the synthesis, if we have developed a sufficient theoretical

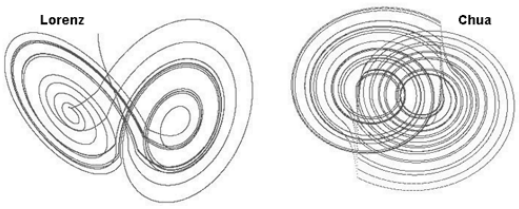

Figure 2: In this figure we present morphologically equivalent Lorenz and Chua attractors from [1].

foundation for a morphological approach.

As an aside, one might ask "why does chaos behave like this?" The answer is that in order for many copies of the same species to evolve it must be possible for a set of approximate operations to be applied to an average set of components in a manner that assures that an average result will be obtained over a sufficiently short time frame. The statistical features of chaos are perfect to carry out this task. Due to the nature of *Nature*, it is advantageous that the operations not be required to be applied in a ridged order, which would make them unadaptable to changes in the environment. A specific chaotic process may apply its operations in a varying order and still obtain the same average result regardless of the initial conditions. So the fact that chaotic systems produce random looking time series for a specific species or brain wave, etc., the morphological results are still similar for each species or process and this is all that is necessary.

We now turn to the problem of understanding the source(s) of the morphology of chaos. We begin with a look at the source of morphology from chaotic equations with discrete forcing or discrete transitions since they provide the easiest method of obtaining insights.

3 The Morphology of Chaos

Both discrete transitions and discrete forcing have been investigated in a series of papers by Brown [1] and Brown and Chua [3-11] Chua, Brown, and Hamilton [12], Brown, Berezdivin and Chua [3] and its relationship to iterated equations and functions, Brown [2], Brown, Brown, and Schlesinger [4]. We draw on those results in the following discussion.

Discrete forcing is illustrated by the equation

$$\dot{\mathrm{X}} = \mathrm{F(X)} + f(t) \tag{1}$$

where it is understood that the variable X is a vector and the forcing function $f(t)$ is discrete, such as $f(t) = \mathrm{sgn}(\cos(t))$ As an example, we can form the discretely forced Ueda equation

$$\ddot{x} + 0.05\dot{x} + x^3 = 7.5 \cdot \mathrm{sgn}(\cos(t))$$

By dropping the damping term we get

$$\ddot{x} + x^3 = 7.5\text{sgn}(\cos(t))$$

Splitting this equation into two we get

$$\ddot{x} + x^3 = 7.5 \quad (2)$$
$$\ddot{x} + x^3 = -7.5 \quad (3)$$

While we have removed the damping term and thus an attractor is no longer present, chaos is still present as demonstrated in the above referenced articles. In particular, the chaos in the discretely forced Ueda equation can now be seen as the composition of the actions of two autonomous components applied successively according to the cadence supplied by the cosine function. With this understanding, we can now introduce simplifications that enable us to construct an equation with all of the chaotic properties of the Ueda equation, but for which the time one map can be explicitly found. The simplest example is the twist-and-flip equation originally published in Brown's dissertation in 1990:

$$\begin{pmatrix} \dot{x} \\ \dot{y} \end{pmatrix} = f(r) \begin{pmatrix} 0 & 1 \\ -1 & 0 \end{pmatrix} \begin{pmatrix} x - a \cdot \text{sgn}(\sin(\omega t)) \\ y \end{pmatrix} \quad (4)$$

where f is an arbitrary function and $r = \sqrt{(x - a \cdot \text{sgn}(\sin(\omega t))^2 + y^2}$.

While this equation may seem strange, it does reveal how discrete equations operate. In particular, it reveals how a chaotic equation cycles through a set of arcs in an almost random fashion to produce a time series. A cadence is set by the frequency of the forcing function and on this cadence, a different arc of a periodic function is selected and used in the time series. What is also revealed is that the morphology is determined by the underlying set of integral curves of the associated autonomous equations. For example, if the sgn of sine is positive then we have the autonomous equation:

$$\begin{pmatrix} \dot{x} \\ \dot{y} \end{pmatrix} = f(r) \begin{pmatrix} 0 & 1 \\ -1 & 0 \end{pmatrix} \begin{pmatrix} x - a \\ y \end{pmatrix} \quad (5)$$

where f is still the same and Eq.4, an arbitrary function, and $r = \sqrt{(x-a)^2 + y^2}$.

The solution of the autonomous equation is straight forward since the function f is constant on integral curves.

$$\begin{pmatrix} x(t) \\ y(t) \end{pmatrix} = \exp(f(r_0) \cdot \text{B} \cdot t) \begin{pmatrix} x_0 - a \\ y_0 \end{pmatrix} \quad \text{and} \quad r_0 = \sqrt{(x_0 - a)^2 + y_0^2} \quad (6)$$

and the matrix B is

$$\begin{pmatrix} 0 & 1 \\ -1 & 0 \end{pmatrix}$$

This equation is called a twist because it twists a straight line into a spiral. With some algebra, we can show that the time-one map of the forced equation is the square of a composition of the above twist followed by a reflection that sends the point (x, y) to the point $(-x, -y)$, also called a 'flip'. Hence, in this case of symmetry, one can generate a random selection of arcs from the twist equation combined with the flip without squaring the composition of the twist and flip. Note that, in the discrete case, it is trivial to string these arcs together in a smoothe manner with a slight adjustment to the discrete forcing function to make it $\mathbf{C}_\infty$ and still retain its essential dynamical properties. In the case of continuous forcing, chaos can be modeled by selecting an infintessimal segment from a family of curves. To see this consider the following argument: Given

$$\frac{d^2x}{dt^2} = F(\frac{dx}{dt}, f(x)) + g(t)$$

we form the approximation

$$\frac{d^2x}{dt^2} = F(\frac{dx}{dt}, f(x)) + a_i, \qquad t \in [t_i, t_{i+1}]$$

or in vector form,

$$\frac{dX}{dt} = F(X) + g(t)$$

From this we form the family of vector equations by using a discrete approximation of the forcing function.

$$\frac{dX}{dt} = F(X) + a_i, \qquad t \in [t_i, t_{i+1}]$$

where,

$$a_i = g(\frac{t_i + t_{i+1}}{2})$$

clearly, from the above decomposition, we can see that from the discrete equation we obtain a selection of arcs from a family of curves from autonomous ODE's. As this approximation is made more accurate, the solution converges to a selection of points from a set of continuously changing curves. We note that just as in the case of the twist equation above, the discrete approximate solution is obtained by forming the composition of the solutions of a family of autonomous equations.

A second case is illustrated by the Chua equation. By carrying out an analysis as done in [1] we reveal the inner workings of this equation. What is shown is that the dynamics can be reduced to something similar to the twist with one modification. The cadence that drives the selection of arcs from

the family of autonomous equations is replaced by a transition surface that serves the same function.

$$\begin{pmatrix} \dot{x}(t) \\ \dot{y}(t) \\ \dot{z}(t) \end{pmatrix} = \begin{bmatrix} \alpha(b+1) & \alpha & 0.0 \\ 1.0 & -1.0 & 1.0 \\ 0.0 & -\beta & 0.0 \end{bmatrix} \begin{pmatrix} x - k\,\mathrm{sgn}(x) \\ y \\ z + k\,\mathrm{sgn}(x) \end{pmatrix}$$

The transition surface is the y, z plane.

In these examples we see that chaotic systems with some form of discrete forcing or transitions can be decomposed into simple linear and nonlinear parts. While chaotic dynamical systems come in many forms as seen in the above references, these examples show that there are at least two distinct classifications possible that provide extensive insight into how chaos works: Those systems which alternate between components through the use of a transition surface such as Chua's double scroll, and those which transition on a cadence such as the Ueda equation and twist-and-flip equations. The meaning of the nonlinear components and how they account for the morphology of a chaotic dynamical systems can be seen by taking a closer look at some decompositions. But before that, a further observation is in order. Most chaotic systems contain both chaotic dynamics and non chaotic dynamics. The well known KAM island chains are an example. The fact that chaotic systems represent healthy heart and brain signals raises the question of whether, under some circumstances, the almost periodic components seen in the KAM island chains can also occur in those signals, and if so, what do they mean? How this might occur is suggested by the Ueda equation. If the damping were to change, then the attractor might settle into an almost periodic orbit. It would be important to understand what physiological forces were at work if this were to happen and what would be the meaning for the patient.

4 Decompositions of Chaotic Systems

From the analysis above, we can gain a great deal of insight by looking at some examples. If

$$\dot{\mathrm{X}} = \mathrm{F(X)} + g(t)$$

we need to first look at the equation

$$\dot{\mathrm{X}} = \mathrm{F(X)} + a$$

where a is a constant. This equation may have damping (or not), and non zero divergence (or not). These conditions will have a significance to the possibilities for time series solutions that depend on the initial condition. A particularly interesting example is illustrated by Figure 4:

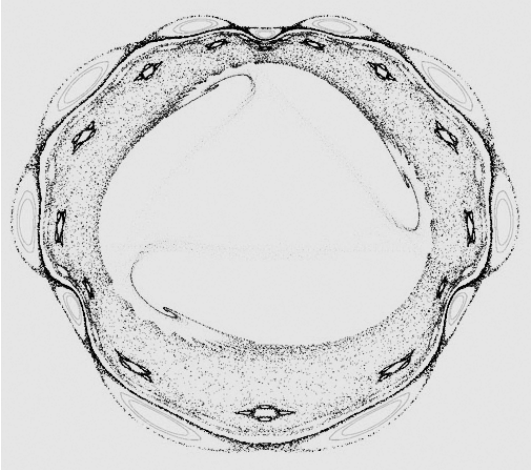

Figure 3: In this figure we see chaotic solutions (light blue and yellow) wrapping around KAM island chains. Because of the nonzero divergence there are three period-three points (red) that are attractors.

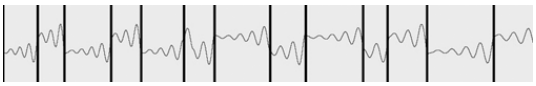

Figure 4: In this figure we show how segments of the Chua-Lorenz type attractor can be recognized and partitioned to facilitate reverse engineering.

In Figure 4 we present a segment of the time series of the y-component of a Chua-Lorenz-type attractor from Brown[1]. We have partitioned the time series into segments that correspond to the components of the attractor. From this partition, we may select the segments corresponding to one of the two components of the attractor and construct an approximation to this component.

After reconstructing each component, we may collect the transition points from the ends of the segment and form an approximate transition surface and then reconstruct the entire attractor in a morphological sense. While this is an "approximation" that will not produce the same time series components in the same order, the reconstruction is sufficient to understand the underlying dynamics. Depending on the application, these underlying component dynamics can be associated to physical or physiological processes. In the case where we are searching for pathologies in a medical application or human EEG or EKG, it is not necessary to reconstruct the entire attractor, but only the components. Understanding pathologies in the time series would thus be reduced to understanding pathologies in the components of the time series. Where these components have been associated to physiological processes, a

remedy strategy may be formulated that may more directly lead to recovery or rehabilitation.

While the composition equation is not an approximation of the solution of the continuous time differential equation (as noted earlier, it does not have to be), it does provide insight into the complex dynamics of the continuous time differential equation and may be used to gain an understanding of the source of the morphology of the continuous time ODE. Approximations of the time series of continuous time chaotic equations is now replaced by understanding the component dynamics that produce the time series morphology of the continuous time equations. As noted above, in the case of human EEG and EKG, the dynamics are common to all 'normal' subjects even though their particular presentation may vary to some degree. This variability is essential for humans to have common skills and understanding while differing in physiology and anatomy, i.e., without each human having to be an exact copy of some standard human being. Hence, we may understand the broad dynamics by decomposing them into simpler, non chaotic autonomous parts from which the general morphology dynamics are derived. The point is that the nonlinear, non chaotic parts are the invariants of the process because they are the source of the morphology even thought they, in combination, produce an ever changing time series. It is important to recall that these "familiar characteristics" pose no obstacles to understanding or using the systems that produce chaotic time series. So we must look to the invariants (non chaotic components) of the system and ask what is their significance.

5 Complex Waves

We have seen that the source of much of chaotic dynamics can be viewed as composed of two elements: A cadence function such as periodic forcing, and a family of periodic curves that have their genesis in an autonomous system. We now look closer at continuous forcing functions. To do this we first revisit the Ueda, equation:

$$\ddot{x} + \delta\dot{x} + \alpha x^3 = \gamma \cos \omega t$$

Based on our analysis of discrete forcing, we know that embedded in this simple equation is a recipe for complex wave motion that might be used to model a wide range of time series such as the EEG and the EKG.

To identify the recipe, or model, for producing complex waves suggested by the Ueda equation we must understand what is essential in the equation to produce complex waves. As noted above, after some analysis the following equation is discovered to contain all of the ingredients needed to produce complex waves.

$$\ddot{x} + \alpha x^3 = \gamma \cos \omega t$$

Our simplification removes the linear damping factor which we know cannot be the source of the complexity in this case. What the damping factor can do is reveal the presence of a strange attractor which we now know to shadow an

underlying unstable manifold. The shape of the unstable manifold accounts for the shape of the strange attractor when there exist a transverse homoclinic point because of the complex manner it must wind about in a finite area as a result of the transverse homoclinic point. The key to the complexity of the solutions of the Ueda equation therefore lies only in the nonlinear factor x^3 and the external forcing function. As the forcing function is periodic and linear, we turn to understanding the nonlinear factor. What we find is that the nonlinear factor introduces in the solution of the Ueda equation is a set of closed curves of varying frequencies and amplitudes. What the cosine forcing introduces is a means of slightly modifying and moving between these curves in a continuous manner. We can reproduce these features using equations that are simpler to analyze. The following equation provides all of the features we are seeking:

$$\ddot{x} + z(x, \dot{x}) \cdot x = \gamma \cos \omega t$$

We note that the Ueda equation is just a special case of this equation where $z(x, \dot{x}) = x^2$ We will call this equation the complex wave equation, or the CWE. From the analysis in the preceding section, we know that the function z and the forcing function *cosine* account for the chaotic properties of the time series. We also know that there is no need to understand the time series exactly. We only need to know that equations of this type can produce chaos, or complex wave phenomena. Hence, in the analysis of time series, we need methods to discover the forcing functions and the function z. To lay the ground work for time series analysis we now analyze the CWE.

There are special cases of this equation that allow us to get a closer look at the dynamics. In particular the case where

$$\dot{z}(x, \dot{x}) = 0$$

is a useful study. The constraint imposed by the above equation allows us to solve the homogeneous version of the equation $\ddot{x} + z(x, \dot{x}) \cdot x = 0$ in closed form in terms of elementary functions since it states that z is constant on integral curves. Like the Ueda equation, the CWE provides a rich set of integral curves with varying frequencies and amplitudes. The cosine forcing assures that the solutions of the inhomogeneous equation are constructed in a manner analogous to the Ueda equation. We will derive a solution for the function z from a first order PDE in a later section and show how similar the dynamics are to those of the Ueda equation.

6 The CWE and the Laws of Physics

The Duffing equation, from which the Ueda equation is formed, is derived by use of the laws of physics. As we will see in the following section, the CWE is derived without the use of the laws of physics. This raises an interesting

question about this approach. Can the brain be modeled by using the laws of physics directly or are the dynamics of the brain so complex that there is little possibility of deriving a model using this approach? All results so far suggest that a new approach is needed. As mentioned above, the approach we have chosen follows the approach used by physicians in diagnosing patient pathologies by use of the EEG or EKG. The physician's approach is to examine the morphology of the EEG/EKG for phenomena that are deviations from the normal from a morphological point-of-view. Hence we have approached the derivation of our model from the point-of-view of obtaining dynamics that fit morphological constraints rather than the constraints of the laws of physics.

7 Morphological Approach to the Derivation of the CWE

In this section we revisit some of the ideas of Sec.5 in order to have a complete discussion of this section topic. As noted above, by a morphological approach we mean that we are seeking to discover the dynamics of a class of equations on the basis of their time series having certain features. This is procedure of dynamical synthesis. In place of using the laws of physics to derive an equation governing a class of dynamics, we examine the time series output of the system and ask what class of equations (type of dynamics) can generate such time series. Through this method we hope to bypass the complex process of deriving brain dynamics from first principles, such as the laws of science, and discover indirectly what those laws are through understanding what equations of motion can generate the complex time series output of the relevant dynamical system.

Our starting point is the simple, linear, harmonic oscillator $\ddot{x} + \lambda^2 x = 0$. This is the simplest possible equation describing how a single point, located at position x riding up and down on a "wave". In this equation, the parameter λ is a constant, representing the frequency of the motion, and is independent of the initial conditions. Hence if we force this oscillator with a periodic function such as $\cos(t)$ only simple almost periodic waves appear except in the case where we have resonance.

As a first step to understanding nonlinear oscillators and how they generate complex wave motion, we look at a two-dimensional simplified version of an ideal fluid rotating about a point(a system derived from the Naiver-Stokes equation). This system of two interconnected ODE's is given by

$$\begin{pmatrix} \dot{x} \\ \dot{y} \end{pmatrix} = r \begin{pmatrix} 0 & -1 \\ 1 & 0 \end{pmatrix} \begin{pmatrix} x \\ y \end{pmatrix} \tag{7}$$

where $r = \sqrt{x^2 + y^2}$. The solution of this equation is

$$\begin{pmatrix} x(t) \\ y(t) \end{pmatrix} = \begin{pmatrix} x_0\cos(rt) + y_0\sin(rt) \\ y_0\cos(rt) - x_0\sin(rt) \end{pmatrix}$$

where $r = \sqrt{x_0^2 + y_0^2}$. Nonlinearity imples that the initial conditions occur in the solution in a nonlinear manner. In this case, the initial conditions determine the frequency of the solution and this frequency is different on each integral curve. In constast, the simple harmonic oscilator has the same frequency on each integral curve. In other words, the frequency of the simple harmonic oscilator is independent of the integral curve and thus it is independent of the initial conditions.

If Eq.7 is driven by a periodic force we obtainthe equation:

$$\begin{pmatrix} \dot{x} \\ \dot{y} \end{pmatrix} = r \begin{pmatrix} 0 & -1 \\ 1 & 0 \end{pmatrix} \begin{pmatrix} x \\ y \end{pmatrix} + \begin{pmatrix} a\cos(t) \\ 0 \end{pmatrix} \tag{8}$$

a complex wave form can arise which is different for each initial condition. In fact, we know that there are chaotic solutions for this equation. In this case, the Fourier Spectrum is of very little value. Where we must look is at the function $r(x, y)^2 = x^2 + y^2$. There are ready generalizations such as

$$\begin{pmatrix} \dot{x} \\ \dot{y} \end{pmatrix} = f(r) \begin{pmatrix} 0 & -1 \\ 1 & 0 \end{pmatrix} \begin{pmatrix} x \\ y \end{pmatrix} + \begin{pmatrix} a\cos(t) \\ 0 \end{pmatrix}$$

Where $r^2 = x^2 + y^2$ and f is an arbitrary function of r. In analogy with the Eq.7, the information lies in the function $f(r)$, not the Fourier Transform. In some sense the function f defines the induced spectrum of the solution set since in the homogeneous unforced case, f is the frequency of the oscillator for a given initial condition. The effect of the forcing function is to move the resultant oscillator over a subset of frequencies defined by the function f. The possible solutions run from periodic to chaotic.

Now consider the following equations:

$$x(t) = x_0\cos(r_0 \cdot t) + \dot{x}_0\sin(r_0 \cdot t)/r_0 \tag{9}$$

$$\dot{x}(t) = \dot{x}_0\cos(r_0 \cdot t) - r_0 x_0\sin(r_0 \cdot t) \tag{10}$$

where $r_0(x_0, \dot{x}_0)$ is some function of the initial conditions. If we assume that $r = r_0$ is a constant of motion, then we can show easily that

$$\dot{x}^2 + r^2 \cdot x^2 = \dot{x}_0^2 + r_0^2 \cdot x_0^2 = C$$

For $C > 0$, this is an equation in the phase plane for an ellipse. Also, note that we can replace r by any positive function of r, $f(r)$. By differentiating the above phase plane ellipse we get:

$$\ddot{x} + r^2 \cdot x = 0$$

or more generally.

$$\ddot{x} + f(r)^2 \cdot x = 0$$

so that this is a nonlinear equation for periodic motion.

Setting $C = r^4$ for convenience of solving the phase plane equation for r, then $r^2 = 0.5(x^2 + \sqrt{x^4 + 4 \cdot \dot{x}^2})$. We take only the positive value of the quadratic equation in r^2 to retain periodic solutions. Other solutions are possible. For example, we may use the following equation to solve for r,

$$\dot{x}^2 + r^2 \cdot x^2 = r^4 + r^2$$

Given the elliptic equation we can now form the forced elliptic equation:

$$\ddot{x} + r^2 \cdot x = a \cdot \cos(t)$$

and obtain chaotic solutions. More properly, we know that the time-one map of this equation has periodic, almost periodic and chaotic solutions due to the presence of KAM island chains.

We now write the above equation in another notation for convenience of illustrating the key ideas:

$$\ddot{u} + z(u, \dot{u}) \cdot u = 0$$

If $\dot{z} = 0$ then z is a constant along integral curves and in particular, $z(u, \dot{u}) = z(u_0, \dot{u}_0) = z_0$. From this know that the solution is given by

$$u(u_0, \dot{u}_0, t) = u_0 \cos(z_0 t) + \dot{u}_0 \sin(z_0 t)/z_0$$

for the integral curve defined by the initial conditions $u_0, \dot{u}_0$, and the frequency is defined by z_0.

In order to see how general this type of "wave" equation is we use both the second order equation and the condition that $\dot{z} = 0$ as a system of equations to solve for the function z. Thus we have

$$\ddot{u} + zu = 0 \qquad \text{and} \qquad \dot{z} = 0 = z_u \dot{u} + z_{\dot{u}} \ddot{u} = 0$$

Eliminating $\ddot{u}$ using both equations we get the following PDE:

$$\dot{u} z_u - u z z_{\dot{u}} = 0$$

Making a change of notation to simplify the picture we get

$$y z_x - x z z_y = 0$$

or

$$yp - zxq = 0$$

a quasi linear homogeneous first order PDE for z. The general solution can be written as either

$$z = f(zx^2 + y^2)$$

or

$$g(z) = zx^2 + y^2$$

hence there exist an uncountable family of solutions for z and likewise there are an uncountable set of nonlinear, periodic ODE's which satisfy these conditions if we require $z > 0$ or what is the same thing, rewrite the equation using z^2 in place of z.

A further generalization comes when we use the form

$$\ddot{u} + z(u, \dot{u}) \cdot u^{2k+1} = 0$$

Solving the relevant PDE for z we get an implicit equation for z as before

$$z = f((k+1)\dot{u}^2 + z \cdot u^{2k+2})$$

Replacing z with z^2 we may obtain the following quadratic equation in z^2 as an example solution.

$$z^4 = (k+1)\dot{u}^2 + z^2 \cdot u^{2k+2}$$

Since z is constant along integral curves, this defines a family of closed curves in the plane.

The above examples serve to demonstrate that the CWE has a very rich range of complex solutions and provides a starting point for deriving morphological dynamics for complex time series.

8 Complex Wave Models

As discussed in the previous section, the simplest complex wave model can be obtained by using following equation:

$$\ddot{u} + z^2 \cdot u = f(\lambda \cdot t)$$

with the constraint $\dot{z} = 0$ and where f is a periodic function. In this equation, z defines an invariant in that the only frequencies possible in the solution must come from the arcs of the functions induced by z.

There are two important properties of the CWE. One is the "clock" or cadence defined by the periodic forcing function and the other is the "spectrum" induced by z. Once we use empirical data to determine the clock and the spectrum, then anomalies from these invariants must signal pathologies or variances in the underlying dynamics that the model represents.

Using the CWE to model the EEG suggests that the brain is not solely a self organizing system as a unit, but that there exists an executive function within the brain which may be self organizing while also being determined by genetics. In particular, the spectrum function and the clock may be genetically determined. These two structures may be the source of the dynamics needed to move neurons into configurations needed by the brain to

learn, repair, and act. A long-term goal is to be able to identify these executive physiological structures by first identifying the 'analytical' spectrum and clock through numerical analysis. Once the analytical spectrum and clock are identified numerically and physiologically, a clearer notion of pathology may be possible to define. In particular, it may be possible to automatically detect when the analytical or physiological EEG spectrum or clock is deviating from the normal or it may be possible to detect when the associated physiological components are changing based on various scanning methods. All of this may be possible to do far sooner than can presently be done by visual examination of the EEG.

9 The Formalization of the Concept of Morphology

In this section we provide a start at formalizing the concept of morphology. Morphology is not a subject of topology or any other area of rigorous mathematics and hence there is no mathematical framework for asking and answering questions about morphology today. What is needed is an initial framework from which to work. An approach is suggested by considering the set of uniformly bounded continuous functions on the real line having uniform bound B. From a morphological point-of-view, we intuitively require that $\sin(x)$ and $\cos(x)$ be the same function, hence, we would like our definition to assure us that $\sin(x) \sim \cos(x)$ And more generally, for any $f \in \mathbf{C}(\mathbf{R})$ and $a \in \mathbf{R}$ we require that $f(x) \sim f(x+a)$. Hence, we have $f \sim g$ relative to a given partition of $\mathbf{R}$, $\{E_i\}$, consisting of finite half open intervals of the real line, $\{E_{j(i)}\}$, where j is a one-to-one and onto mapping of the integers (note that this implies that $E_{j(i)} = E_i + a_i$ for some real number a_i) and $f(x) = g(x + a_i)$ on the interval E_i. This means that the function g is a translation of f partition wise, but not necessarily globally.

Using this definition we see that $\sim$ defines an equivalence relation on $\mathbf{C}(\mathbf{R})$. By considering $\mathbf{C}(\mathbf{R})$ mod this equivalence relation, we from the morphology space, $\mathcal{M}_B$.

In general, in order to compare two functions, f, g, morphologically, we must do so relative to a given partition of $\mathbf{R}$, call it $\{E_i\}$. We proceed by selecting a one-to-one, onto mapping of the integers,j and form the partition $\{E_{j(i)}\}$ (which provides a set of real numbers a_i), we compare f on the partition element E_i to g on the element $E_i + a_i$ by forming the number $|f(x) - g(x + a_i)|$. This clearly provides a notion of the degree of closeness of f and g for each pair of partition elements, $E_i, E_{j(i)}$. The maximum absolute difference of f and g over all such partition element pairs provides a notion of morphological closeness of the two functions over the entire given partition of $\mathbf{R}$. Now, by considering all possible partitions of $\mathbf{R}$ and selecting the one for which f and g are the closest, we get a notion of how close g is to f in a morphological sense.

We may now define a notion of closeness formally for a function $f \in \mathcal{M}_B$. Given $f \in \mathcal{M}_B$, for any $g \in \mathcal{M}_B$, define

$$d(f,g) = \liminf_{\mathbf{P}}(\sup_{E_i \in \mathbf{P}} |f(x) - g(x + a_i)|)$$

Clearly, $d(f,f) = 0$, $d(f,g) = d(g,f)$, and $d(f,g) \geq 0$. To prove that this notion of closeness is actually a metric we must prove that $d(f,g) \leq d(f,h) + d(h,g)$ which is beyond the scope of this paper.

Associated to any ODE is a morphology space formed by the set of all solutions of the ODE. We may now partition the domain of initial conditions into equivalent classes according to the morphology space. Hence, two initial conditions are equivalent if the time series generated by the two initial are morphology equivalent. Further, the initial conditions are close if their time series solutions of the ODE are morphologically close.

10 Dynamical Synthesis

In [1] and [6] we began a program called *dynamical synthesis*. While the above analytical considerations are useful in moving this program forward, we demonstrate in this section that the considerations in the previous sections are nowhere nearly enough to set the stage for a formal program seeking to discover the full range of dynamics possible in nature. While the principle of dynamical synthesis is to recognize that the underlying physical forces driving many dynamical systems may be so complex (i.e., EEG's, tornados) that there is little hope of deriving their mathematical formulation from first principles, or from either the classical of modern laws of the physics; because the objective of dynamical synthesis is to discover the underlying physical principles in complex systems by observing a physical phenomena and reverse engineering the dynamics by 'guessing' what dynamics might produce such a system, we need an investigation into the sources of complexity in mathematical and physical systems by constructing a broad array of examples and counterexamples analogous to those found in [8] in particular. To set the stage, we provide an illustration from [8] that demonstrates the power of combining, in a simple weighted sum, a periodic process with a Bernoulli process (in particular an Anasov flow on a tour).

If we were to start from the laws of physics, it would be difficult to arrive at this figure which is suggestive of natural processes. However, by knowing how this figure is derived, it may make it easier to model real natural processes by starting with a weighted sum of periodic and complex motions that are known to exist within the environment of interest.

We now show how to construct complex time series that produce stretching and folding such as occurs in chaotic dynamical systems, and what may be called subchatoic behavior such as illustrated in [8]. In order to advance this line of investigation, we seek to discover the types of time series (as opposed

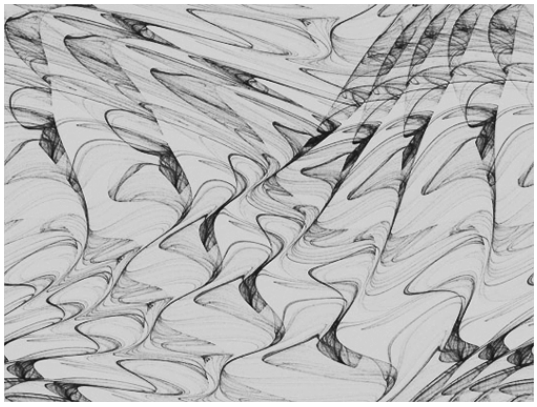

Figure 5: This figure, reproduced from [8] is a simple weighted sum $w \cdot B + (1-w) \cdot P \quad 0 < w < 1$ of a Bernoulli system and a Periodic system.

to differential equations) that may generate unstable manifolds, complex torsion, pseudo random behavior and generally, any complex behavior beyond almost periodic processes. In what follows, we present examples of time series that produce images that resemble the unstable manifolds of chaotic dynamical systems and bifurcations to chaos as well as complex high dimensional dynamics. In order to generate complex time series we must resort to using implicit functions and very small step size finite differences with step sizes on the order of 10^{-3}.

Since explicit time series of chaotic solutions of ODE's seems out of reach at present, we turn to implicit functions that bifurcate to chaos. Phase plots constructed from bifurcating implicit functions provide an insight into the structure of complex systems generally.

Implicit functions of the form $x(t) = f(x(t), t)$ have a relationship to finite difference equations of the form $x(t+h) = f(x(t), t)$. Specifically, if one were to seek to solve the implicit function equation by simple iteration, the solution to the associated finite difference equation (AFDE) is the first iterate. For implicit functions that can be solved by simple iteration, the solution of the AFDE will converge to the implicit function. For implicit functions that have hyperbolic fixed points, this does not happen.

The class of FDE's we will use are those that have a non trivial associated implicit function (AIF). In particular we only consider equations of the form:

$$x(t+h) = f(x(t), t) \tag{11}$$

$$\frac{\partial f}{\partial h} = 0 \tag{12}$$

The condition

$$\frac{\partial f}{\partial h} = 0$$

eliminates equations arising from numerical approximations of differential equations. The reason that we eliminate this form of FDE is that they do not reveal the inner workings of chaotic ODE's. For example, how the forcing function of the Ueda equation constantly changes the frequency of the solution function is not clear from its conventional Taylor series approximation as demonstrated in the following equation:

$$\begin{aligned} x(t+h) &= x(t) + h \cdot y(t) && (13) \\ y(t+h) &= y(t) + h(a \cdot \cos(t) - \alpha \cdot y(t) - x(t)^3) && (14) \end{aligned}$$

The associated implicit function is degenerate. Hence as our starting point, we have selected the cosine function:

$$x(t) = C_0 \cos(x(t)) \quad (15)$$

The solution to this equation is a fixed point for which the repelling points are of the most interest. To create a time series we add an inhomogeneous term. For this we choose the most manageable way forward by adding a simple periodic term in the argument of the cosine. We include an arbitrary constant to be determined by the initial condition, Eq. 16 below. The reason we have chosen this approach is that typical differential equations that produce chaos can be driven by periodic functions which constantly changes the frequency of the solution curve as discussed in Sec. 4. In general, the continuous time solutions to Eq.17 and FDEs require knowing the function on an interval $[0, h)$, not just at two points $x(0), x(h)$.

$$x(t) = C_0 \cos(x(t) + a \sin(t)) \quad (16)$$

We now shift to a finite difference expression having a small step size where h can be made as small as we like. h will be the step size used in generating the time series. The specific choice of our starting point is based on the analysis in Sec. 3,4 and Sec. 5 which demonstrates that we must have continuously changing frequency to have any chance of deriving time series that are chaotic and that frequence must change in a nonlinear manner.

$$x(t+h) = C_0 \cos(x(t) + a \sin(t)) \quad (17)$$

The constant C_0 can be evaluated by setting $t = 0$. Doing this we get

$$C_0 = \frac{x(h)}{\cos(x_0)} \quad (18)$$

Clearly, there are two datum needed to complete this formula which may or may not converge to an implicit equation for the unknown function $x(t)$.

The implicit equation is solved by finding the fixed points, for each t, for the map:

$$T_t(x) \quad = \quad C_0 \cos(x + a \sin(t)) \tag{19}$$

The derivative of this map tells what type of fixed point we have.

$$DT_t|_x \quad = \quad -C_0 \sin(x + a \sin(t)) \tag{20}$$

For $|C_0| < 1$ we have contracting fixed points, signaling that the finite difference equation will have 'nice' solutions for all values of t. However, when $|C_0| > 1$, the solutions of the implicit function equation can be hyperbolic, depending on the value of $\cos(x(t) + a \sin)t))$, and, if so, will pose problems of numerical analysis.

Interestingly, it is the hyperbolic fixed points of Eq.16 that play a significant role in the construction of complex time series of Eq.17. In particular, for a hyperbolic fixed point of Eq.16, the iterates of Eq.16 will be repelled from the fixed point. But, the first iterate is precisely $x(t + h)$. Hence, we have the following situation: For contracting fixed points, $x(t+h)$ is attracted toward the solution of Eq.16, and for hyperbolic fixed points, $x(t + h)$ is repelled away from the solution of Eq.16. The solution of Eq.16 is thus always exerting a force on all associated finite difference equations. Specifically, as $|C_0| \to \infty$, the hyperbolic fixed points of Eq.16 bifurcate to produce a period doubling sequence of attracting periodic points. It is this period doubling process that is the key to the complexity of the time series from Eq.17. In other words, how this relates to the finite difference equation with any step size is that the dynamics of the time series that the finite difference equation generates is driven by the associated period doubling process of the implicit equation. This situation is illustrated in a series of figures below.

In the following 5 time series illustrated below, the value of the arbitrary constant goes from ≈ 0.94 to ≈ 1.94. In the top time series all fixed points of the associated implicit function (AIF) are all attracting creating a very simple continuous time series. For the second time series (red) $c \approx 1.44785$ and we see that the time series has bifurcated in accordance with the AIF. The bifurcation is to a pair of attracting period two points. The time series values alternate between these two period two points producing a discontinuous function. The function could be made continuous by selecting the same period-two branch of the bifurcation diagram of the AIF. The green time series shows a period-four bifurcation; the dark blue is period 8 and the light blue is a very high period bifurcation. The value of the constant a is 6 in all figures. The step size is ≈ 0.0008

A remarkable fact of this bifurcation process is that the discontinuity of the time series is the source of the 'order' on the dynamics seen in the delay plot in the figures in the next section.

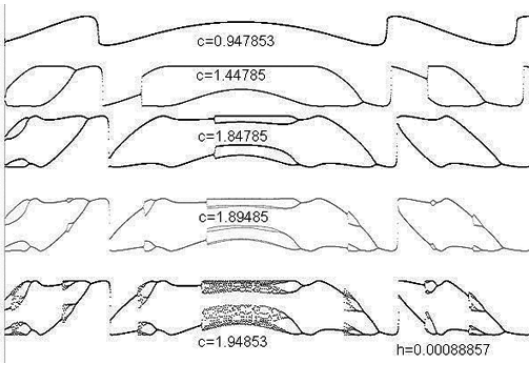

Figure 6: This figure shows the progression of a time series as the associated implicit function bifurcates. It is this bifurcation that plays a role in the derivation of the following equations and associated illustrations.

11 Order Out of Chaotic Bifurcation Diagrams

In this section we present a series of phase diagrams that are generated by short time step finite difference equations such as seen in Eq.17 above. Each value of the parameter h defines a different function so long as the function G is fixed. Hence, if we change the step size in Eq.17, we get a new function, and a new phase plot. Further, as $h \to 0$ the sequence of functions define by Eq.17 do not necessarily converge to the solution of the implicit function equation, Eq.16 .

In Figure 7 below, we use a variation on Eq.17 with $c_0 \approx 1.2, a = 6.0, h \approx 0.008$:

Figure 8 demonstrates that we can obtain near pseudo randomness by choosing a high enough frequency for the cosine functions.

$$\begin{aligned} x(t+h) &= C_1 \cos(x(t) + a \cdot \sin(t)) + C_2 \sin(x(t) & (21) \\ \dot{x}(t+h) &= -C_1 \sin(x(t) + a \cdot \sin(t)) \cdot \dot{x}(t) + a \cdot \cos(t) \\ &+ C_2 \cdot \cos(x(t)) \cdot \dot{x}(t) & (22) \end{aligned}$$

By holding the parameters fixed and modifying the initial conditions we create spiral dynamics. Figures 8 and 9 demonstrate that the dynamics can vary dramatically with the initial conditions. This is also true for ODEs in that a single ODE can produce KAM island chains. While this seems difficult to make sense of at first, we will see in the last section that almost periodic functions and chaotic functions are more closely related than one would expect. We demonstrate that, with these two figure, we can separate the phase space into two main regions between which the system oscillates.

By reducing the value of a from 10 in Fig. 9 and 10 to 3 in Fig. 11 we reduce oscillations and form a single spiral.

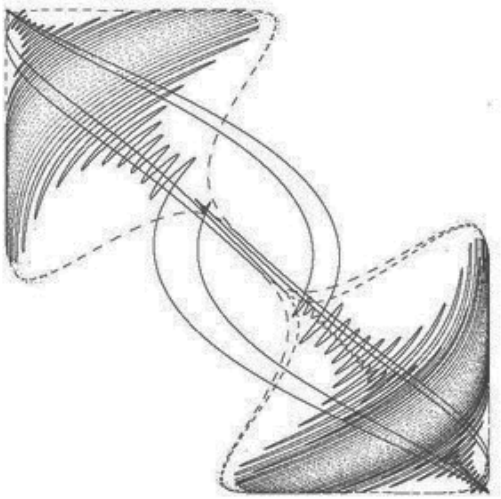

Figure 7: in this figure we use the equation $x(t+h) = c_0 \cdot \cos(x(t)^2 - a \cdot \sin(t))$ which shows the presence of nonlinear oscillations.

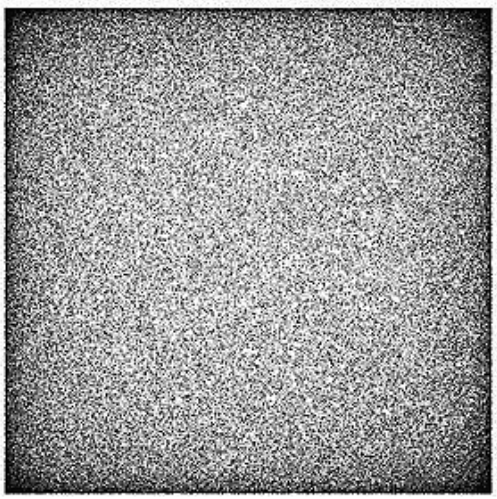

Figure 8: Figure 8 uses Eq.17 with $a = 7000, c_0 = 1.44785, h = 0.0088$.

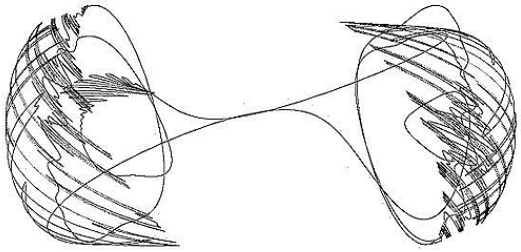

Figure 9: The equations for this figure are Eq.21 and Eq.22. In this figure $C_1 \approx 0.8036, C_2 \approx 2.0, a = 10.0, h \approx 0.0237$.

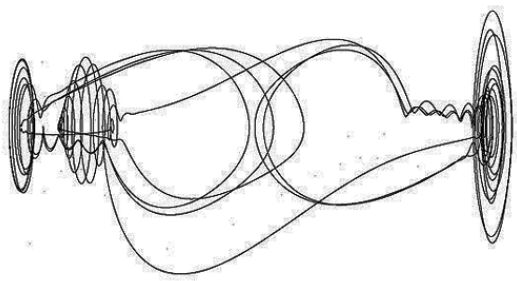

Figure 10: In this figure we use the equations of Fig.9 where $C_1 \approx 0.8783, C_2 \approx 1.7236, a = 10.0, h \approx 0.0237$.

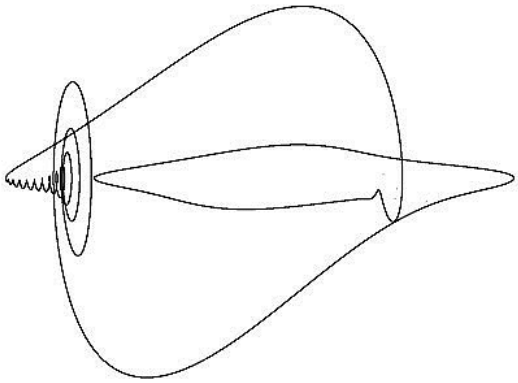

Figure 11: In this figure we also use the same equations as Fig. 8 and 9 with $C_1 \approx 0.8788, C_2 \approx 1.257, a = 3.0, h \approx 0.044$.

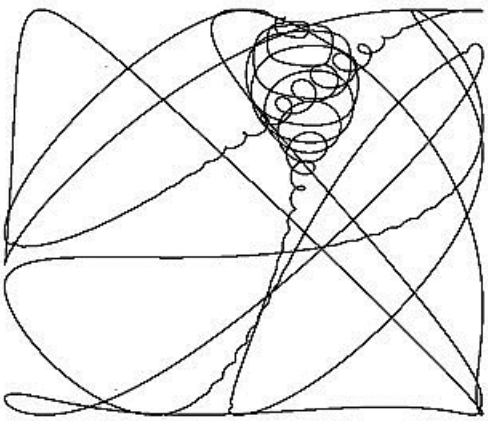

Figure 12: In this figure $C_1 \approx 1.29557, C_2 \approx 1.099750, a = 6.0, h \approx 0.006935$.

We now shift to another equation form in two variables. The arbitrary constants are determined by four initial conditions, making this a four-dimensional system. See Eq.23 and 24 below.

$$x(t+h) = C_1 \cos(y(t) + a\sin(t)) \quad (23)$$
$$y(t+h) = -C_2 \sin(x(t) + a\cos(t)) \quad (24)$$

The dynamics in this figure show the formation of circular motion that develops into a high amplitude rotation before dying out and recycling. In Fig.12 below, we retain the same equations and parameters except that we increase C_2

12 Bifurcation in Phase Plane Dynamics

In the next example we switch from using periodic functions to using rational functions. The phase plane dynamics plot is $(x(t+h), x(t)$. In this series of three illustrations we vary the parameter a causing the phase plane image to bifurcate to what resembles an unstable manifold. We use the following equation:

$$x(t+h) = \frac{7 \cdot x(t)^2}{2 + x(t)^2} + a\sin(3t) \quad (25)$$

In Figures 13-15 we vary the amplitude of the forcing function as shown in each figure.

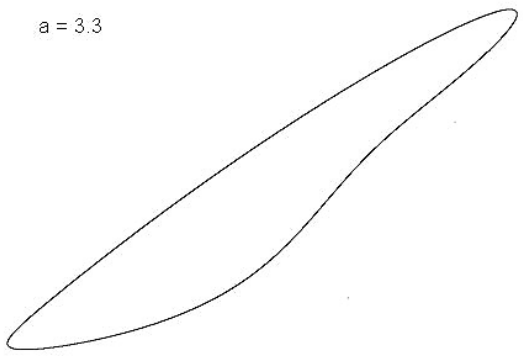

Figure 13: In these figures $a = 3.3, 3.5, 5.68, h \approx 0.0888$.

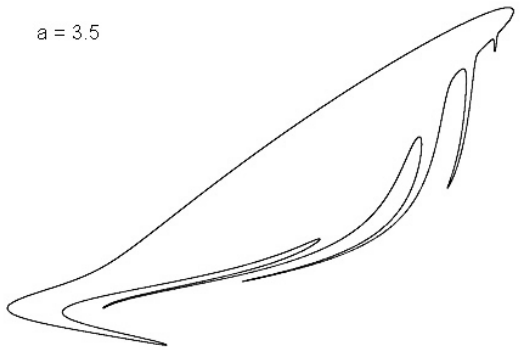

Figure 14: In these figures $a = 3.3, 3.5, 5.68, h \approx 0.0888$.

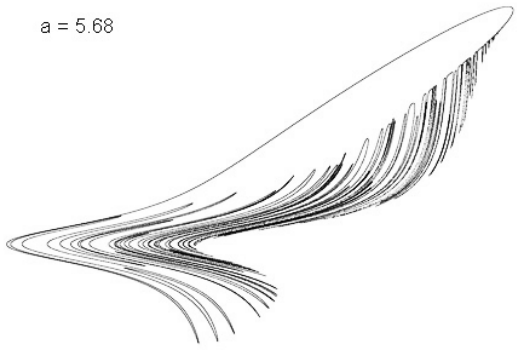

Figure 15: In these figures $a = 3.3, 3.5, 5.68, h \approx 0.0888$.

For this equation we can compute the fixed points directly. What we observe in these three figures is the transition from a simple almost periodic function to a very complex almost periodic function based on changing the parameter a only. .

13 Almost Periodic Approximations to Unstable Manifolds

So far we have been able to progressively develop remarkably high levels of complexity from very simple finite difference equations. However, they are high dimensional examples since the FDE's require more than two values to solve for the arbitrary constants. In this section we show how to generate two-dimensional complexity. In contrast to the equation

$$x(t+h) = \cos(x(t) + a\sin(t))$$

the following equation, derived from the family of twist-and-flip equations, shows the changing frequency and the time series as a finite, explicit expression in terms of elementary functions. If the functions, f, g, h are periodic, then the solutions are almost periodic, and hence not chaotic. However, the integral curves, though almost periodic, bear a strong resemblance to the unstable manifolds of chaotic equations.

$$\begin{pmatrix} x(t) \\ y(t) \end{pmatrix} = \begin{pmatrix} \cos(f(r)) & \sin(f(r) \\ -\sin(f(r)) & \cos(f(r) \end{pmatrix} \begin{pmatrix} c_1 g(t) \\ c_2 h(t) \end{pmatrix} \tag{26}$$

The general form of Eq.26 is

$$\mathrm{X(t)} = \mathrm{A}(f(r))\mathrm{C}(t) \tag{27}$$

Since $\det(\mathrm{A}) = 1$ we have $r^2 = x^2 + y^2 = c_1^2 g(t)^2 + c_2^2 h(t)^2$.

The following is an example of a two-dimensional phase plane integral curve of Eq.27. The explanation for this comes from observing how illustrations of unstable manifolds are derived. See [5].

The ODE is given by

$$\dot{\mathrm{X}} = \dot{r} f'(r)\mathrm{A}'(f(r))\mathrm{A}^{-1}(f(r))\mathrm{X} + \mathrm{A}(f(r))\mathrm{G}(t) \tag{28}$$

If we let

$$\mathrm{B} = \begin{pmatrix} 0 & 1 \\ -1 & 0 \end{pmatrix}$$

Then Eq.28 simplifies to

$$\dot{\mathrm{X}} = \dot{r} f'(r)\mathrm{BX} + \mathrm{A}(f(r))\mathrm{G}(t) \tag{29}$$

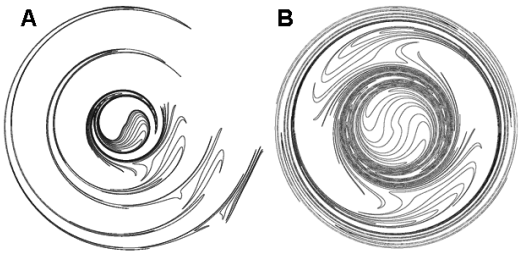

Figure 16: For both A and B $\lambda_1 = 0.2, \lambda_2 = 6.0, c_1 = 20.2, c_2 = 12.0, f(r) = 1/(1.2 + \sin(r))$. In A, we modify g as follows: $g(t) = \cos(\lambda_1 \cdot t) + 1$. h is unchanged from the above description.

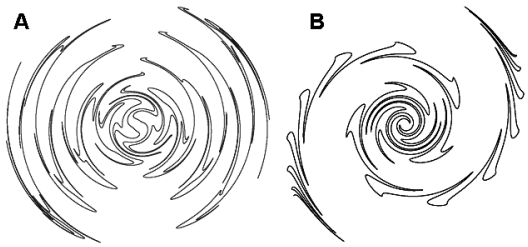

Figure 17: For both A and B $\lambda_1 = 0.2, \lambda_2 = 8.0, c_1 = 55.0, c_2 = 15.0$. In Plate A, $f(r) = \sin(r)$: in Plate B $f(r) = 4\log(r)$.

The presence of the factor $\dot{r}$ means that the Lipschitz condition can fail and we do not have unique solutions for Eq.29. The meaning of this is that, while the unstable manifold of a forced ODE is not, itself, a solution to a well behaved ODE, it may be possible to approximate the unstable manifold by a solution of an ill conditioned ODE such as Eq.26 above. The significance of this is that all of the complexity that arises from chaotic systems may be approximated by almost periodic time series which can be written down in closed form, as a finite expression, in terms of elementary functions. Note that the almost period can be very long, and for all practical purposes, cannot be distinguished from a function which is not almost periodic.

In the figures that follow, $g(t) = \cos(\lambda_1 \cdot t), \quad h(t) = \cos(\lambda_2 \cdot t)$. The function $f(r)$ varies as indicated. The frequency parameters $\lambda_1, \quad \lambda_2$ are specified as are the arbitrary constants. The frequencies, as suggested by Eq.26 should be widely separated. The arbitrary constants $c_1, \quad c_2$ can be equal. Also, the arbitrary constants play the role of both amplitude and frequency, as can be seen from Eq. 26.

In Fig. 18, Plate A is the image of an unstable manifold from the twist-and-flip map [1]. Plate B is the integral curve from Eq.29. As mentioned before, Eq.29 does not have unique solutions. As demonstrated in Figs.

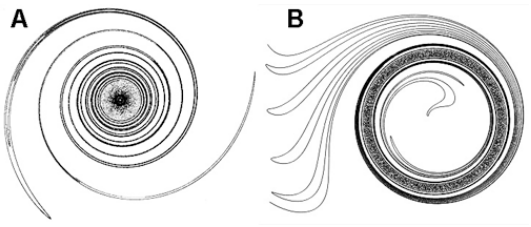

Figure 18: For Plate B $\lambda_1 = 0.2, \lambda_2 = 1.0, c_1 = c_2 = 10.0, f(r) = 2/(\sin((1 + 2r\log(r))/r)$.

6-15, complex time series also arise form bifurcating implicit functions by using the first iterate as a FDE. These observations suggest that there is a relationship between bifurcating implicit functions and ODE's which do not have unique solutions. All equations have common characteristics of varying frequencies connected to an underlying set of integral curves which are invariants for autonomous ODE's such as the autonomous CWE and other Hamiltonian systems. It seems possible that there is a theorem linking all of these factors together and linking the results to chaos, perhaps providing a basis for developing a "theory of chaos".

14 Summary

Chaos has been an elusive phenomena in the sense that precise definitions are difficult as shown in [7,9,10,11]. Moreover, applications have been difficult to formulate because of the inherent unpredictability of chaotic systems. Conversely, models of complex systems have been difficult to derive because the underlying physical principles are difficult to determine. To address these problems we have suggested two changes in our point-of-view. First, view chaos and other complex systems morphologically. Second, approach complex systems through the method of dynamical synthesis. These two concepts are interconnected. We have further demonstrated using these two concepts we can derive a dramatic range of complex dynamics without reference to physical principles. These results suggests the need for a disciplined approach that involves deriving theorems and formal computational techniques to provide a systematic framework for analysis of complex systems. In short, there is a need to develop a new area of mathematical inquiry that classifies, describes, predicts, and explains complexity in a formal, computational setting.

15 References

[1] Brown, R., [1992] Generalizations of the Chua Equations, *IEEE Transactions on Circuits and Systems* 40(11).

[2] Brown, R. [1999], On Solving Nonlinear Functional, Finite Difference, Composition, and Iterated Equations, *Fractals* 1999.

[3] Brown, R., Berezdivin, R., and Chua, L., [2001] Chaos and Complexity, *International Journal of Bifurcation and Chaos* 11(1)

[4] Brown, B., Brown, R, Shlesinger, M., [2003] Solution of Doubly and higher order iterated equations, *J. of Stat. Physics*, Vol. 110, Nos. 3-6

[5] Brown, R. & Chua, L. [1991] "Horseshoes in the Twist-and-Flip Map," *International Journal of Bifurcation and Chaos* **1**(1),235-252.

[6] Brown, R. & Chua, L. [1993] "Dynamical Synthesis of Poincaré Maps," *International Journal of Bifurcation and Chaos***3**(5),1235-1267.

[7] Brown, R. & Chua, L. [1996] "Clarifying Chaos: Examples and Counterexamples," *International Journal of Bifurcation and Chaos***6**(2)

[8] Brown, R. and Chua, L., [1996] From almost periodic to chaotic: The fundamental map *International Journal of Bifurcation and Chaos* 6(6).

[9] Brown, R. and Chua, L., [1997] Chaos: Generating complexity from simplicity *International Journal of Bifurcation and Chaos* 7(7).

[10] Brown, R. & Chua, L. [1998] "Clarifying Chaos II:Bernoulli Chaos, Zero Lyapunov Exponents, and Strange Attractors" *International Journal of Bifurcation and Chaos***8**(1), pp.1-32

[11] Brown, R. and Chua, L., [1999] "Clarifying Chaos III: Stochastic Processes" *International Journal of Bifurcation and Chaos* 9(5).

[12] Chua, L., Brown, R. and Hamilton, N. [1993] "Fractals in the Twist-and-Flip Circuit" Proceedings of the IEEE, Invited Paper.

[13] Poincare, H. [1892]. Les Methodes Nouvelles de la Mechanique Celeste. GauthierVillars, Paris.

[14] Smale S. [1967] Differentiable Dynamical Systems. Bull Am Math Soc **73**:747817.

Received December 2008; revised April 2009.